Passive Earth Pressure with Critical State Concept

Yung-Show Fang[1]; Ying-Chieh Ho[2]; and Tsang-Jiang Chen[3]

Abstract: This paper presents experimental data of earth pressure acting against a vertical rigid wall, which moved toward a mass of dry sand. The backfill had been placed in lifts to achieve relative densities of 38, 63, and 80%. The instrumented retaining-wall facility at National Chiao Tung University in Taiwan was used to investigate the effects of soil density on the development of earth pressure. Based on the experimental data, it has been found that the Coulomb and Terzaghi solutions calculated with the peak internal friction angle significantly overestimated the ultimate passive thrust for the retaining wall filled with dense sand. As the wall movement *S* exceeded 12% of the wall height *H*, the passive earth thrust would reach a constant value, regardless of the initial density of backfill. Under such a large wall movement, soils along the rupture surface had reached the critical state, and the shearing strength on the surface could be properly represented with the residual internal-friction angle. The ultimate passive earth pressure was successfully estimated by adopting the critical state concept to either Terzaghi or Coulomb theory.

CE Database keywords: Passive pressure; Earth pressure; Sand; Vertical angles.

DOI: 10.1061/(ASCE)1090-0241(2002)128:8(651)

Introduction

The most widely accepted theories of earth pressure among practicing engineers are those of Coulomb and Rankine. However, considerable doubt has been expressed regarding the validity of these theories. Several investigations have been conducted to estimate the passive soil thrust P_p. Morgenstern and Eisenstein (1970) compared the passive earth pressure coefficient K_p calculated with theories proposed by Caquot and Kerisel (1948), Brinch-Hansen (1953), Janbu (1957), Sokolovski (1960), and Terzaghi and Peck (1967). It was concluded that Coulomb's theory overestimated passive resistance, and noticeable differences exist between the theories. It should be noted that most of the design charts and tables based on theoretical solutions lack experimental justification.

In Coulomb's theory, it is assumed that the failure surface in the backfill is planar. However, Terzaghi (1941) and Terzaghi et al. (1996) indicated that, due to the influence of wall friction, the real surface of the sliding in the backfill consists of a curved lower part and a straight upper part. As a wall pushes toward the retained backfill, the straight portion of the sliding surface rises at an angle of $45° - \phi/2$ with the horizontal, as shown in Fig. 1(a). The material within the area *ADF* is in the passive Rankine state. The curved part of the surface of sliding *BCD* was assumed to be a logarithmic spiral. The analytical results using this revised failure surface will be termed the Terzaghi method, and it will be compared with experimental data.

Valuable experimental work associated with passive earth pressure has been conducted by Schofield (1961); Rowe and Peaker (1965); Mackey and Kirk (1967); Narain et al. (1969); James and Bransby (1970), Matsuo et al. (1978), Fang et al. (1994; 1997); and Duncan and Mokwa (2001). Mackey and Kirk (1967) reported that if the backfill is loose, the passive earth pressure obtained experimentally compared well with those obtained from Coulomb's theory. However, if the backfill is dense, the Coulomb solution is approximately 100% higher than the experimental results. Narain et al. (1969) reported that the passive pressure coefficient K_p calculated with Coulomb theory is 127% higher than the experimental value. Fang et al. (1994) concluded that the passive pressure distribution is linear and in good agreement with Terzaghi's solution. However, the experimental work by Fang et al. (1994) had been limited to loose cohesionless backfill only. In most specifications for earthwork, the contractor is required to densify the backfill to 90–95% of its maximum dry unit weight determined by the standard Proctor test. For granular soils, achieving a relative density of 70–75% is generally recommended (see the NAVFAC Design Manual) (US Navy 1982) by vibratory compaction. To reduce compaction induced pressure, hand tampers or lightweight equipment are commonly used (Day 1998). Therefore, in most cases, the backfill in the field would be dense soil. Unfortunately, little experimental justification had been provided regarding the validity of passive pressure theories for dense backfill, which is of practical importance to the design engineer.

Behavior of Sand during Shear

It would be logical to infer that the passive earth pressure is related to the shearing resistance of soil along the rupture surface *BCDEF* shown in Fig. 1(a). Holtz and Kovacs (1981) described that, when loose sand is sheared in a triaxial test, the principal stress difference $(\sigma_1 - \sigma_3)$ gradually increases to an ultimate

[1]Professor and Chairman, Dept. of Civil Engineering, National Chiao Tung Univ., Hsinchu, Taiwan 30010, R.O.C. (corresponding author). E-mail: ysfang@cc.nctu.edu.tw

[2]Graduate Student, Dept. of Civil Engineering, National Chiao Tung Univ., Hsinchu, Taiwan 30010, R.O.C.

[3]Ph.D. Candidate, Dept. of Civil Engineering, National Chiao Tung Univ., Hsinchu, Taiwan 30010, R.O.C.

Note. Discussion open until January 1, 2003. Separate discussions must be submitted for individual papers. To extend the closing date by one month, a written request must be filed with the ASCE Managing Editor. The manuscript for this paper was submitted for review and possible publication on March 28, 2001; approved on December 21, 2001. This paper is part of the ***Journal of Geotechnical and Geoenvironmental Engineering***, Vol. 128, No. 8, August 1, 2002. ©ASCE, ISSN 1090-0241/2002/8-651–659/$8.00+$.50 per page.

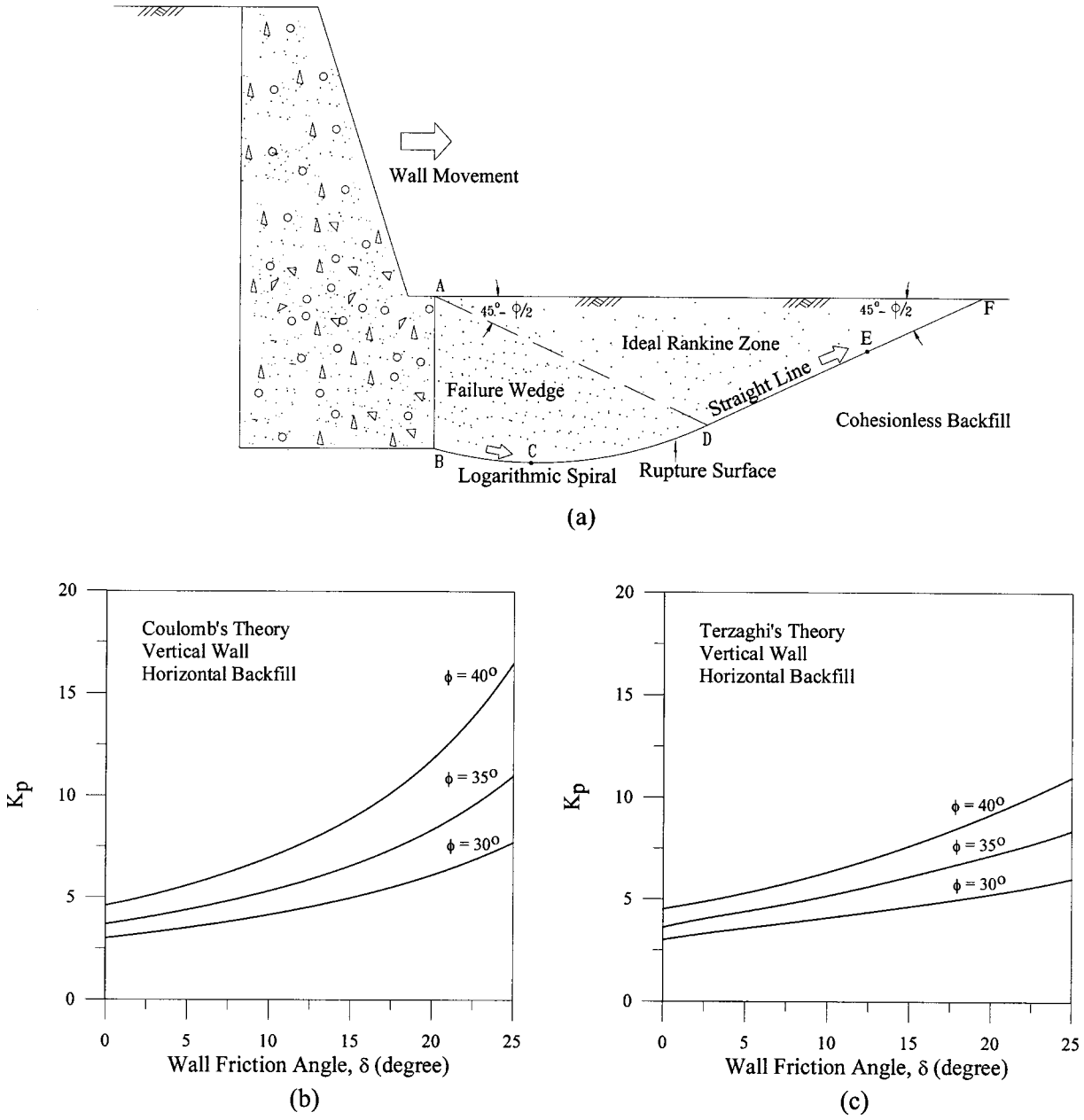

Fig. 1. (a) Passive wedge calculated with Terzaghi's log-spiral method; (b) variation of K_p obtained from Coulomb's theory; and (c) variation of K_p obtained from Terzaghi's theory [(c) redrawn after Das 1990]

value as shown in Fig. 2(a). Concurrently, the volume of the specimen decreases from e_1 (loose) down to a value very close to the critical void ratio e_{crit}. Casagrande (1936) called the ultimate void ratio, at which continuous deformation occurs with no change in principal stress difference, the critical void ratio. This condition is referred to as the ultimate, constant volume, or residual condition (Lambe and Whitman 1969). Lambe and Whitman stated that, in most problems encountered in engineering practice, it is not possible to tolerate large strains within a sand mass. Thus for most problems the value of ϕ based upon the peak of the stress–strain curve is properly used to represent the strength of the sand. However, there are some problems in which large strains occur. For such problems, it would be appropriate to use ϕ_{cv} or ϕ_r to represent the strength of the sand, where the subscript cv and *r* stand for constant volume and residual, respectively.

When a dense specimen is sheared, the principal stress difference reaches a peak value and subsequently decreases to a value very close to $(\sigma_1-\sigma_3)_{\text{ult}}$ for loose sand as shown in Fig. 2(a). The void ratio–stress curve in Fig. 2(b) shows that the dense sand contracts slightly at first, then dilates up to a value very close to e_{crit}. It should be mentioned that the critical void ratio of soil is a function of the confining pressure. It is clear in Fig. 2(b) that, as dense sand dilates with increasing strain, the dense specimen is no longer ''dense.''

The experimental work by Narain et al. (1969) indicates that, considering the translation mode, wall movements needed to reach a passive state for loose and dense fills are as high as 8.9 and 6.8% of the wall height, respectively. Under such large wall deformations, the soil along the rupture surface most probably has reached the critical state. It would be reasonable to expect that, under the passive condition, the shearing resistance of soil along

J. Geotech. Geoenviron. Eng. 2002.128:651-659.

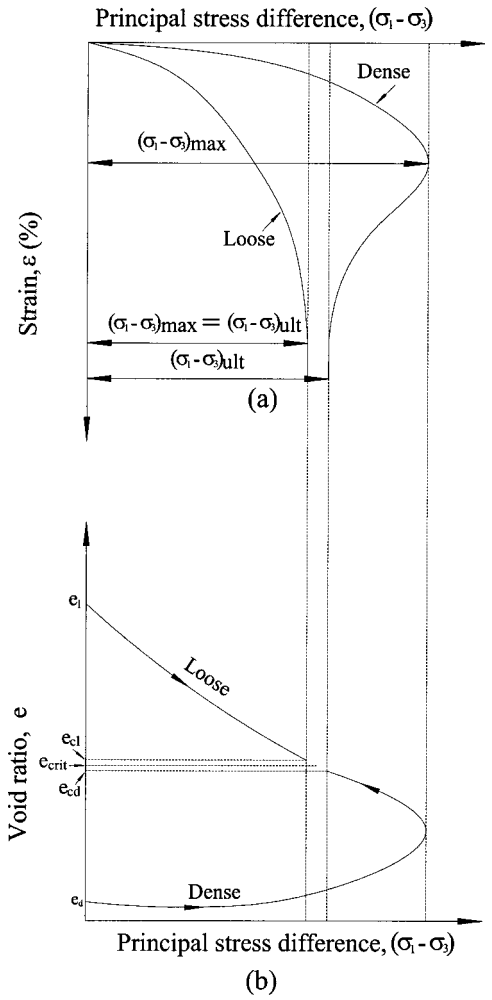

Fig. 2. Triaxial tests on loose and dense specimens of typical sand: (a) stress–strain curves and (b) void ratio changes during shear (Holtz and Kovacs 1981)

the rupture surface has reached the ultimate strength, irrespective of its initial density. If the inference above is correct, it could be expected that the ultimate passive pressure for loose and dense fills would be identical. However, in most earth pressure theories, such as Coulomb's theory, the shear strength of soil was assumed to be a constant.

This paper presents experimental data of passive pressure against a vertical rigid wall, which moved toward a mass of dry sand with a stress-free horizontal surface. To limit the scope of this study, only the translational wall movement was performed to investigate the effect of soil density on passive pressure. Air-dry Ottawa sand had been placed in lifts to reach relative densities of 38, 63, and 80%. All of the experiments mentioned in this paper were conducted in the National Chiao Tung Univ. (NCTU) retaining-wall facility. Horizontal earth pressure against the wall was measured with the soil pressure transducers (SPTs) mounted on the wall. Test data were compared with the well-known Rankine, Coulomb, and Terzaghi theories. Based on the critical state concept, a more rational approach to estimate the passive pressure is proposed.

National Chiao Tung Univ. Retaining-Wall Facility

The entire facility consists of four components: model retaining wall, soil bin, driving system, and data acquisition system.

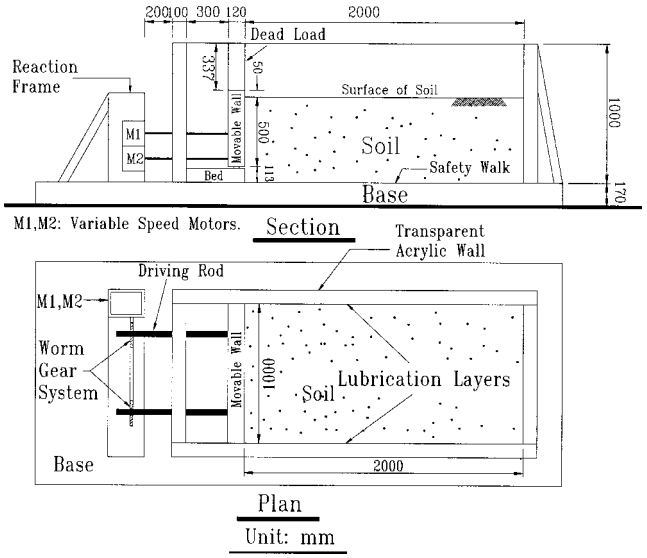

Fig. 3. National Chiao Tung Univ. retaining-wall facility

The movable model retaining wall and its driving system are illustrated in Fig. 3. The model wall is a 1,000-mm-wide, 550-mm-high, and 120-mm-thick solid plate, and is made of steel. Note that in Fig. 3, the effective wall height H (or height of backfill above wall base) is only 500 mm. The retaining wall is vertically supported by two unidirectional rollers, and is laterally supported by four driving rods. The 1,000-mm-wide, 337-mm-high, and 120-mm-thick steel plate on top of the movable wall is designed to resist the uplift component of passive earth pressure. To investigate the distribution of earth pressure, SPTs were attached to the model retaining wall as shown in Fig. 4. Ten strain-gage-type earth pressure transducers have been arranged within the central zone of the wall. Another three transducers (SPT10, SPT11, and SPT12) have been mounted between the central zone and sidewall to investigate the sidewall effect. Fang et al. (1994) reports that when the sidewalls of the soil bin are lubricated, earth pressures measured at different distances from the sidewall are in fairly good agreement. However, because the lubrication of the sidewall does not completely eliminate friction, the passive resistance measured at SPT12 is slightly greater than those measured at SPT6, SPT10, and SPT11. To reduce the soil-arching effect,

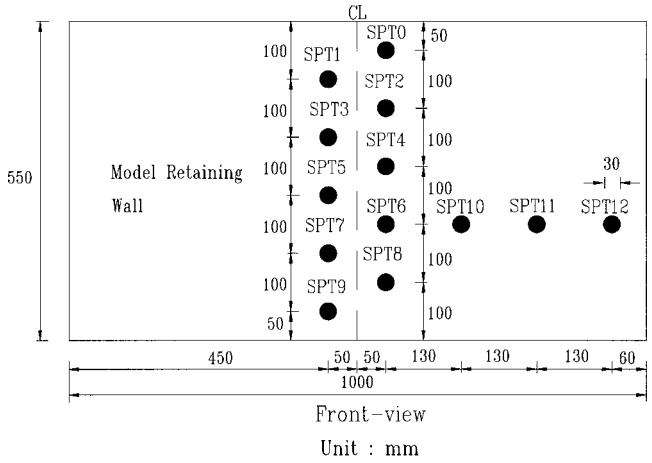

Fig. 4. Locations for soil-pressure transducers

J. Geotech. Geoenviron. Eng. 2002.128:651-659.

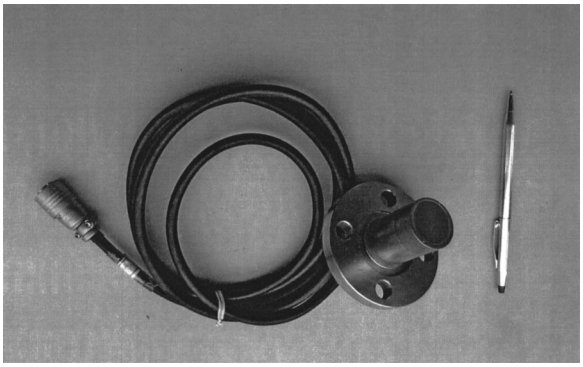

Fig. 5. Soil pressure transducer

earth-pressure transducers with a stiff sensing face are installed flush with the face of the wall. The Kyowa model BE-2KRS17 (196 kN/m^2 capacity) transducer shown in Fig. 5 was used for these experiments.

Dunnicliff (1988) described that, if measurement accuracy must be maximized, each cell should be calibrated in a large calibration chamber, using the soil in which it will be embedded. The chamber should be at least three times, and preferably five times the diameter of the cell. Following Dunnicliff's recommendation, a special device was designed for the calibration of the SPT used for this study. The calibration device is a shallow cylindrical chamber with an inner diameter of 400 mm and a height of 30 mm. The chamber is made of a solid steel plate, which is the same material as the model retaining wall. The surface of the sensor was installed flush with the bottom plate of the chamber and covered with a 10-mm-thick sand layer. A 0.2-mm-thick rubber membrane was placed on top of the sand and a uniform distributed air pressure was applied on the membrane. The output voltage measured by the data acquisition system was found to increase linearly with the increase of applied pressure.

The soil bin is fabricated of steel members with inside dimensions of 2,000 mm×1,000 mm×1,000 mm (see Fig. 3). Both sidewalls of the soil bin are made of 30-mm-thick transparent acrylic plates through which the behavior of backfill can be observed. The bottom of the soil bin is covered with a layer of SAFETY WALK, which is an antislip frictional material, to provide adequate friction between the soil and the base of the bin. According to the general wedge theory (Terzaghi 1941), the passive failure surface developed in the backfill would extend below the base of the wall. As shown in Fig. 3, the fixed bed located below the wall serves to hold the bottom 113 mm of soil to accommodate the entire log-spiral failure surface.

As illustrated in Fig. 3, the variable speed motors M1 and M2 (Electro, M4621AB) are employed to compel the upper and lower driving rods, respectively. The shaft rotation compels the worm gear linear actuators, while the actuator would push the model wall. Since only the variation of earth pressure caused by the translational wall movement is investigated, the motor speeds at M1 and M2 were kept the same for all experiments in this study.

Due to the considerable amount of data collected by the soil-pressure transducers, a data acquisition system was used. An analog-to-digital converter digitized the analog signals from the sensors. The digital data were then stored and processed by a microcomputer. A general view of the NCTU model retaining wall is shown in Fig. 6. For more details regarding the NCTU retaining-wall facility, the reader is referred to Wu (1992a) and Fang et al. (1994).

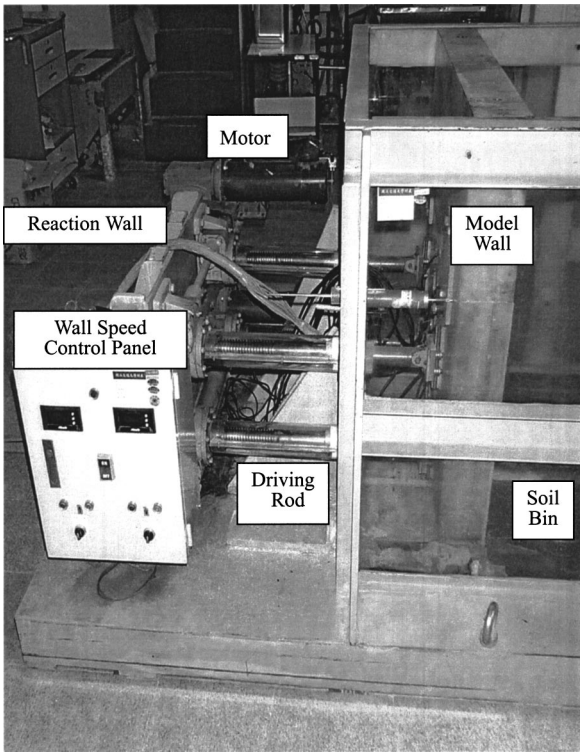

Fig. 6. National Chiao Tung Univ. model retaining wall

Backfill and Interface Characteristics

Air-dry Ottawa sand (ASTM C-109) was used throughout this investigation. Physical properties of the soil include $G_s=2.65$, $e_{max}=0.76$, $e_{min}=0.50$, $D_{60}=0.36$ mm, and $D_{10}=0.23$ mm. To investigate the effects of soil density on passive pressure, the backfill was prepared at three different densities. The relative density obtained for loose, medium dense, and dense backfill was 38, 63, and 80%, respectively. To achieve the loose condition, the backfill was deposited by air pluviation from the slit of a hopper into the soil bin. The drop distance was approximately 1.0 m from the soil surface throughout the placement process.

As illustrated in Fig. 3, the total thickness of backfill in the soil bin was 613 mm. To obtain the expected medium dense and dense conditions, the loose backfill was placed in five lifts. Each lift was pluviated into the soil bin, carefully leveled, then compacted with a vibratory compactor. The soil surface was divided into several lanes and each lane was densified with the soil compactor with a 90 s pass. The soil compactor shown in Fig. 7 was made by fixing an electric motor (Mikasa Sangyo, KJ75-2P) to a steel plate. The total mass of the soil compactor is 12.1 kg. A number of steel plates were attached eccentric to the central rotating shaft of the motor to control the vibratory compaction applied to the soil surface. Based on the results from density control tests, six and sixteen eccentric plates were used to achieve the medium dense and dense backfill, respectively.

Density control cups were used to evaluate the variation of soil density in the soil mass. The cylindrical cup was made of acrylic with an inner diameter of 100 mm and height of 50 mm. For the density distribution experiment, the cups were buried in each lift before compaction. After the entire backfill had been densified, the cups were extracted and the unit weight of soil in the cup was determined. It was found that the soil density was quite uniform in the soil mass. Data obtained from five dense backfill tests in-

J. Geotech. Geoenviron. Eng. 2002.128:651-659.

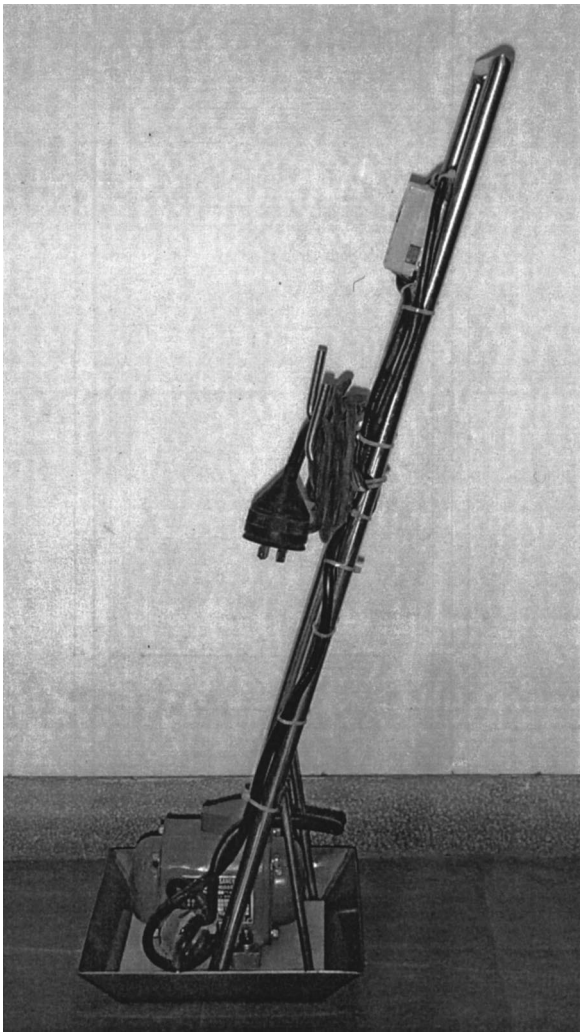

Fig. 7. Vibratory soil compactor

dicated that the standard deviation of relative density with depth was only 0.3%. However, it should be mentioned that the uppermost cup was placed at 123 mm below the soil surface. It is possible that low unit weight might exist in the top lift due to the vibration and lack of confinement in the sand.

Direct shear tests were conducted to determine the internal friction angle ϕ of the loose, medium dense, and dense backfill. The entire shear box was placed in the soil bin, pluviated with Ottawa sand, subjected to the compaction effort, extracted from the soil mass, and tested in the laboratory. The peak and residual ϕ angles determined for the sand at different densities are summarized in Table 1. The interface friction angle δ between the backfill and model wall was obtained by replacing the lower shear box with a smooth steel plate, to simulate the surface of the model wall. Uesugi and Kishida (1986) investigated the friction between steel and air-dry sands with a simple shear apparatus. It was found that the peak and residual interface friction angles are the same because the model wall had a smooth surface. For the case of a rough wall surface, a peak friction angle higher than the residual angle was reported. The ϕ and δ angles determined from the tests were adopted to calculate earth pressures from the Coulomb and Terzaghi theories in the following sections.

Table 1. Parameters for Loose, Medium Dense, and Dense Backfill

Backfill, condition	Unit weight γ (kN/m^3)	Relative density D_r (%)	Peak internal friction angle ϕ_{peak} (deg)	Residual internal friction angle ϕ_r (deg)	Wall friction angle δ (deg)
Loose	15.7	38	33.0	31.5	9.8
Medium dense	16.3	63	38.3	31.5	12.6
Dense	16.8	80	42.1	31.5	14.0

Based on Coulomb and Terzaghi theories, the variation of passive earth-pressure coefficient K_p computed with varying ϕ and δ angles are shown in Figs. 1(b and c) for the case of a level ground surface and a vertical wall. Considering relatively low δ angles, the values of K_p determined from both theories are nearly the same. However, considering relatively high δ angles, the values of K_p determined from Coulomb and Terzaghi theories, are very different. In this study, the model wall is made of steel and the δ angle adopted in this study varies from 9.8 to 14.0°. Thus the test results and conclusions obtained are only applicable for relatively low values of wall friction angles.

To reduce the friction between sidewall and backfill, a lubrication layer was furnished for the earth-pressure experiments. The layer consists of a 0.2-mm-thick latex rubber membrane and a thin layer of silicone grease (Shin-Etsu KS-63G). Tatsuoka and Haibara (1985) found that, if the normal stress is greater than 40 kN/m^2, the friction angle at the interface could be successfully reduced to less than 1°. The rubber membrane-grease method has been used by Wu (1992b); Huang et al. (1994), Fang et al. (1994; 1997); and other researchers for large-scale model tests.

Test Results

This section reports on the effects of soil compaction on passive earth pressure against a rigid wall. For all experiments, the surface of backfill was horizontal and the height of the backfill above the wall base H was 0.5 m.

Wall with Loose Backfill

The variation of lateral earth pressure as a function of passive wall movement was investigated. After the loose backfill had been placed into the soil bin, the model wall slowly moved toward the soil mass in translational mode at a constant speed of 0.24 mm/s. No compaction was applied to the loose backfill.

Distributions of horizontal earth pressure σ_h measured at different stages of wall displacement S/H are illustrated in Fig. 8. As the wall started to move, the earth pressure increased, and eventually a limiting passive pressure was reached. The pressure distributions are essentially linear at each stage of wall movement. Passive earth pressure calculated with Coulomb and Terzaghi theories is also indicated in Fig. 8. The ultimate experimental passive pressure distribution is in fairly good agreement with that estimated with Coulomb and Terzaghi theories.

The variation of horizontal earth-pressure coefficient K_h as a function of wall displacement is shown in Fig. 9. The coefficient K_h is defined as the ratio of the horizontal component of total trust to $\gamma H^2/2$. The horizontal thrust P_h was calculated by summing the pressure diagram shown in Fig. 8. The coefficient K_h increased with increasing wall movement until a maximum value was reached, then remained approximately constant. The ultimate value of K_h is defined as the horizontal passive earth-pressure

J. Geotech. Geoenviron. Eng. 2002.128:651-659.

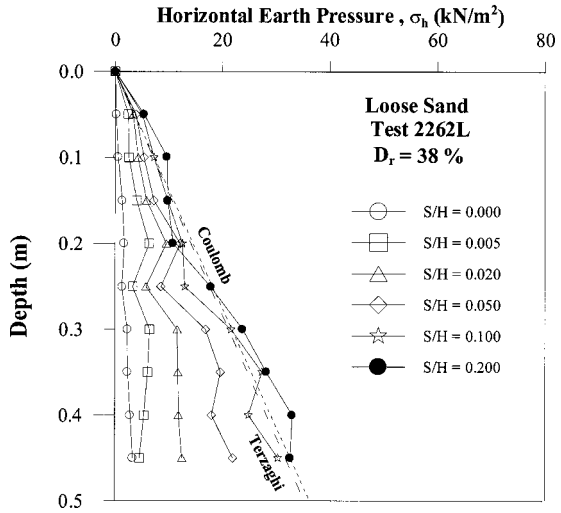

Fig. 8. Distribution of lateral earth pressure for loose sand

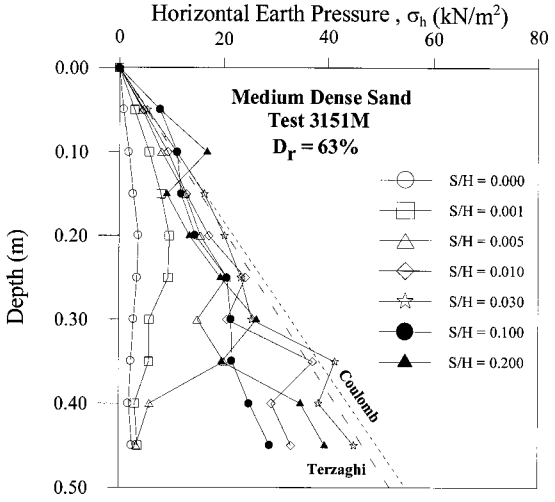

Fig. 10. Distribution of lateral earth pressure for medium dense sand

coefficient $K_{p,h}$. In Fig. 9, the passive condition was reached at approximately $S/H=0.17$. It may be observed from Fig. 8 that both Coulomb and Terzaghi theories provide a good estimate of the passive thrust against the retaining wall with a loose backfill. However, Rankine theory tends to underestimate the passive earth pressure. This is most probably due to the fact that Rankine theory discounts the friction effect between the wall surface and backfill. In Fig. 9, data points obtained from Tests 2262L, 3042L, and 3043L indicate that the experimental results were quite reproducible.

Wall with Medium Dense Backfill

After the backfill had been compacted to the relative density of 63%, the model wall moved as a solid block toward the backfill. Fig. 10 illustrates the distributions of earth pressure at different stages of wall movement. The earth pressure measured near the base of the wall (SPT7, SPT8, and SPT9) increased with increasing wall movement before reaching a peak value. After the peak, σ_h decreased with further wall displacement. The wall movement needed for σ_h to reach a peak value was about $S/H=0.03$. However, the earth pressure measured by the transducers near the top of the backfill (SPT1 and SPT2) did not decrease with increasing wall movement. This is probably because loose sand (low unit weight) might exist in the top lift of the backfill.

Fig. 11 shows the variation of coefficient K_h as a function of wall movement. The lateral soil thrust increases with increasing wall movement until a maximum value is reached, then K_h decreases with further wall movement. The peak value is slightly lower than the passive coefficients $K_{p,h}$ estimated with the Terzaghi theory with the peak friction angle ϕ_{peak}. However, with further wall movement, the coefficient K_h decreases, then reaches an ultimate value. The ultimate condition for the medium dense backfill is reached at approximately $S/H=0.10$. Under such a large wall displacement, it is reasonable to expect that the soil elements at points *C*, *D*, *E*, and *F* in Fig. 1(a) have dilated and reached the critical state. For this reason, the passive earth-pressure coefficients $K_{p,h}$ based on Coulomb and Terzaghi theories were calculated with the residual internal friction angle ϕ_r and are indicated in Fig. 11. The experimental ultimate K_h values are in fairly good agreement with Coulomb and Terzaghi's predictions calculated with the residual friction angle.

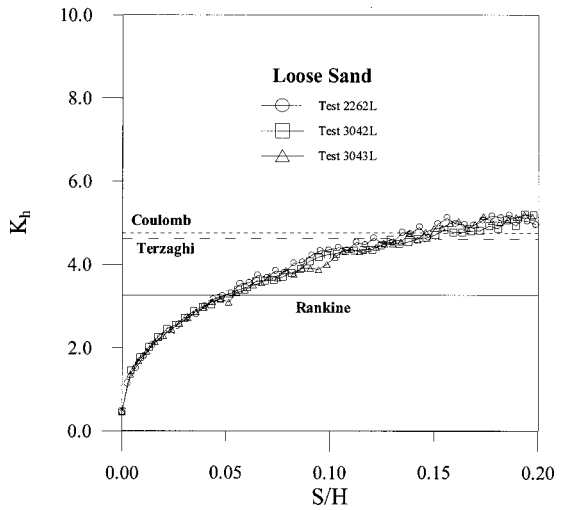

Fig. 9. Variation of K_h with wall movement for loose sand

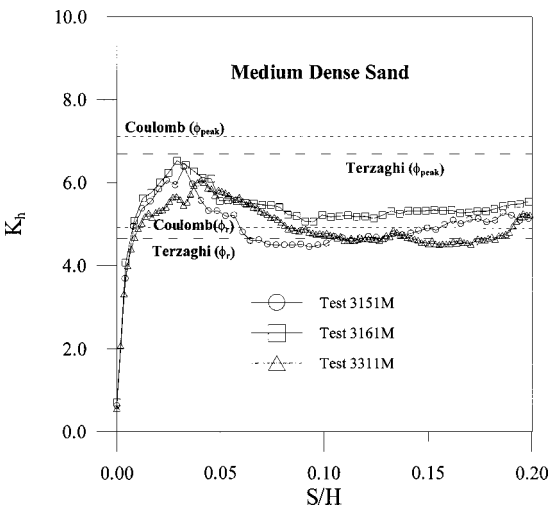

Fig. 11. Variation of K_h with wall movement for medium dense sand

J. Geotech. Geoenviron. Eng. 2002.128:651-659.

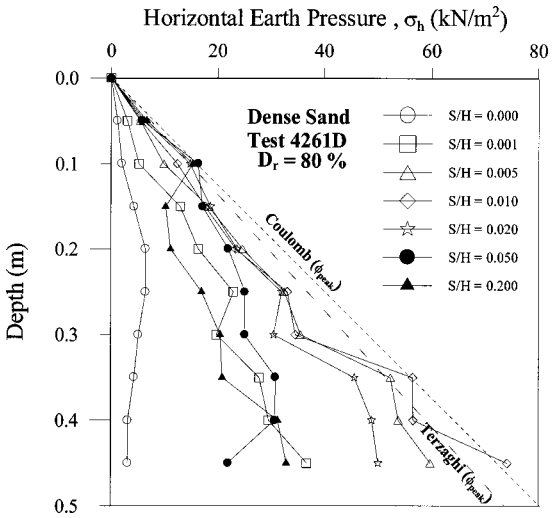

Fig. 12. Distribution of lateral earth pressure for dense sand

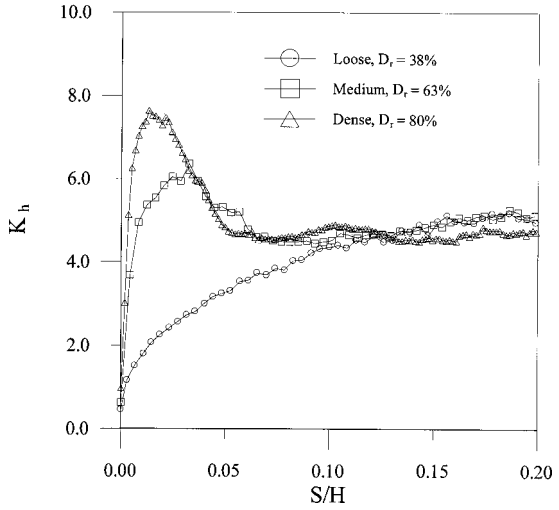

Fig. 14. Variation of K_h with wall movement for loose, medium dense, and dense backfill

Wall with Dense Backfill

The distributions of earth pressure at different stages of wall movement are shown in Fig. 12. The horizontal pressure measured at Transducer SPT9 initially increased with increasing wall movement. A peak pressure was reached at approximately $S/H = 0.01$, then the pressure decreased with further wall movement. Eventually, a stable earth pressure was achieved. Similar pressure change could be observed at Transducers SPT3–SPT8. The passive pressure distribution under a large wall movement, for example $S/H = 0.20$, was much less than that estimated with the classic Coulomb and Terzaghi theories.

In Fig. 13, the earth-pressure coefficient K_h initially increased with increasing wall movement. After reaching a peak value, K_h decreased with increasing passive wall movement, and finally reached an ultimate value. The traditional Coulomb and Terzaghi solutions calculated with a constant ϕ_{peak} angle significantly overestimated the ultimate passive thrust. However, at a large wall movement, the ultimate K_h value could be properly estimated by introducing the critical state concept to the traditional Coulomb and Terzaghi theories.

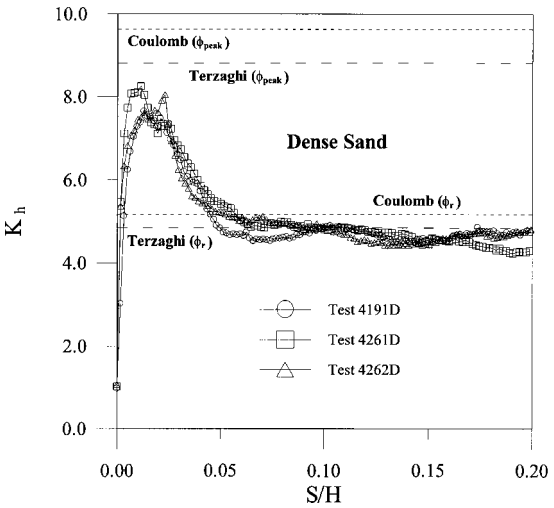

Fig. 13. Variation of K_h with wall movement for dense sand

Effect of Soil Density on Earth Pressure

The effects of soil density on earth pressure can be easily interpreted with the help of Figs. 1(a) and Fig. 2. Fig. 1(a) shows the retaining wall, passive soil wedge, and failure surface. Based on Terzaghi's general wedge theory, as the retaining wall would push toward the dense backfill, the dense sand along the logarithmic–spiral curve *BC* would be sheared, and the soil density would decrease. After passing the peak strength, as indicated in Fig. 2, the shearing resistance would decrease with volume expansion. Eventually, an ultimate strength would be reached. Under a large shear strain condition, the initially ''dense'' sand would no longer be dense, and the friction angle ϕ_{peak} would no longer be an appropriate strength parameter.

With the reduction of shearing resistance along the *BC* surface, the passive earth pressure against the wall would decrease. With continued wall movement, the rupture surface would extend progressively through points *C*, *D*, *E*, and *F*. In the process, soil elements along the rupture surface would dilate, change strength, and eventually reach a critical state.

Fig. 14 shows the variation of experimental earth-pressure coefficient K_h with wall movement for loose, medium-dense, and dense backfill. For the dense backfill, the soil thrust initially increased rapidly with small increments of passive movement. After reaching a peak value, the coefficient K_h dropped down until a constant value was reached. For the loose backfill, K_h increased with increasing wall displacement until a steady state was reached. For the medium-dense backfill, the pressure value varied between that for loose and dense backfill. The wall movement needed for K_h to reach a peak value was about 0.015 *S/H* for dense sand, and about 0.03 *S/H* for medium dense backfill. It should be noted that, as the passive wall movement *S/H* exceeded 0.12, the passive soil thrust would approach a constant value regardless of the initial density of backfill. It may be concluded that the soils along the rupture surface had reached the critical state, and the shearing strength on the surface could be properly represented with the residual ϕ_r angle.

Fig. 15 shows the theoretical and experimental passive earth-pressure coefficients $K_{p,h}$ versus soil density. Two groups of experimental $K_{p,h}$ are plotted in this figure. One group represents the peak thrust, and the other represents the ultimate passive thrust obtained at a large wall displacement. For comparison pur-

J. Geotech. Geoenviron. Eng. 2002.128:651-659.

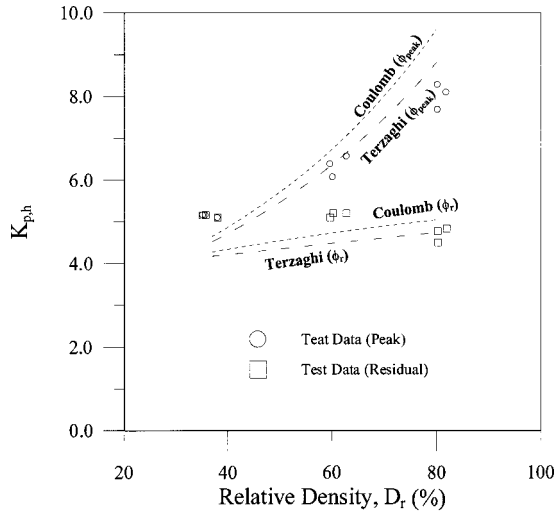

Fig. 15. Variation of $K_{p,h}$ as a function of soil density

poses, the classic Coulomb and Terzaghi solutions are also plotted in this figure. For the loose backfill, the Coulomb and Terzaghi theories slightly underestimated the passive thrust. For walls with medium dense and dense backfill, the peak experimental results were in good agreement with Terzaghi's solution calculated with ϕ_{peak}. If the residual ϕ_r angle was considered with the Coulomb and Terzaghi theories, the theoretical solutions were found to be in relatively good agreement with the experimental ultimate passive thrusts.

Design Recommendation

Based on the test results obtained in this study, a recommendation on the estimation of passive earth pressure behind a retaining wall is proposed. As indicated in Fig. 1(a), passive pressure is often presumed to resist the active movement of the wall. An overestimation of the passive resistance would indicate an overestimated factor of safety against sliding, that would put the design on the unsafe side. When calculating the passive earth pressure, it is recommended that one considers the dilation and subsequent strength reduction of dense backfill. The passive earth pressure at a large wall displacement can be successfully approximated by introducing the critical state concept to either Terzaghi or Coulomb theory. This reasonable and conservative design would be more likely to keep the retaining wall on the safe side.

Conclusions

Based on the experimental data obtained during the investigation, the following conclusions can be drawn about the development of passive earth pressure against a rigid wall that translates toward a dry cohesionless backfill:

1. For the wall with loose backfill, the earth pressure increased with increasing wall movement, and eventually reached a limiting passive pressure. The pressure distribution at each stage of wall movement was essentially linear.
2. For the wall with dense backfill, the earth pressure coefficient K_h increased with increasing wall movement. After reaching a peak value, K_h decreased with increasing wall movement, and finally reached an ultimate value. The Coulomb and Terzaghi solutions calculated with the ϕ_{peak} angle significantly overestimated the ultimate passive thrust.
3. As the wall movement *S/H* exceeded 0.12, the passive soil thrust would reach a constant value, regardless of the initial density of backfill. It may be deduced that soils along the rupture surface had reached the critical state, and the shearing strength on the surface could be properly represented with the residual ϕ_r angle.
4. For the wall with a loose backfill, Coulomb and Terzaghi's theories slightly underestimated the passive thrust. For walls with medium dense and dense backfill, the peak experimental results were in good agreement with Terzaghi's solution calculated with ϕ_{peak}. Considering the relatively low δ angles adopted in this study, the Coulomb and Terzaghi theories were found to be in relatively good agreement with the experimental ultimate thrusts, when passive earth pressures were computed on the basis of the residual shear strength parameter ϕ_r.
5. When calculating the passive earth pressure, it is recommended that one considers the dilation and the strength reduction of dense backfill. The ultimate passive earth pressure could be successfully approximated by introducing the critical state concept to either Terzaghi or Coulomb theory.

Acknowledgments

The writers wish to acknowledge the National Science Council of the Republic of China government (Grant No. NSC 88-2611-E-009-007) for the financial assistance that made this investigation possible. Special thanks are extended to Mr. Shin-Yu Chang and Chien-Ting Chen for their assistance.

References

Brinch-Hansen, J. (1953). *Earth pressure calculation*, Danish Technical Press, Copenhagen, Denmark.

Caquot, A., and Kerisel, J. (1948), *Tables for the calculation of passive pressure, active pressure, and bearing capacity of foundations*, Gauthier-Villars, Paris.

Casagrande, A. (1936). "Characteristics of cohesionless soils affecting the stability of slopes and earth fills." *J. Boston Civ. Eng., January, reprint in Contributions to Soil Mechanics*, 1925–1940, ASCE, 257–276.

Das, B. M. (1990). *Principles of foundation engineering*, 2nd Ed., PWS-Kent, Boston.

Day, R. W. (1998). "Discussion of 'earth pressure with sloping backfill,' " *J. Geotech. Geoenviron. Eng.*, 124(11), 1152–1153.

Duncan, J. M., and Mokwa, R. L. (2001). "Passive earth pressures: theory and tests." *J. Geotech. Geoenviron. Eng.*, 127(3), 248–257.

Dunnicliff, J. (1988). *Geotechnical instrumentation for monitoring field performance*, Wiley, New York.

Fang, Y. S., Chen, J. M., and Chen, C. Y. (1997). "Earth pressures with sloping backfill." *J. Geotech. Geoenviron. Eng.*, 123(3), 250–259.

Fang, Y. S., Chen, T. J., and Wu, B. F. (1994). "Passive earth pressures with various wall movements." *J. Geotech. Eng.*, 120(8), 1307–1323.

Holtz, R. D. and Kovacs, W. D. (1981). *An introduction to geotechnical engineering*, Prentice-Hall, Englewood Cliffs, N.J.

Huang, C. C., Cheng, C. Y., Hsia, S. H., and Hsu, S. P. (1994). "Reinforcement stiffness on load-deformation characteristics of reinforcement." *Proc., 5th Int. Conf. on Geotextiles, Geomembranes and Related Products*, Singapore, 187–200.

James, R. G., and Bransby, P. L. (1970). "Experimental and theoretical investigations of a passive pressure problem." *Geotechnique*, 20(1), 17–37.

J. Geotech. Geoenviron. Eng. 2002.128:651-659.

Janbu, N. (1957). ''Earth pressure and bearing capacity calculations by generalized procedure of slices.'' *Proc., 4th Int. Conf. on Soil Mechanics and Foundations Engineering, London, 207–212.*

Lambe, T. W., and Whitman, R. V. (1969). *Soil mechanics*, Wiley, New York.

Mackey, R. D., and Kirk, D. P. (1967). ''At rest, active and passive earth pressures.'' *Proc., South East Asian Conf. on Soil Mechanics and Foundations Engineering*, Bangkok, 187–199.

Matsuo, M., Kenmochi, S., and Yagi, H. (1978). ''Experimental study of retaining wall by field tests.'' *Soils Found.*, 18(3), 27–42.

Morgenstern, N. R., and Eisenstein, Z. (1970). ''Methods of estimating lateral loads and deformations.'' *Proc., ASCE Speciality Conf. on Lateral Stresses in the Ground and Design of Earth-Retaining Structures*, Ithaca, N.Y., 51–102.

Narain, J., Saran, S., and Nandakumaran, P., (1969). ''Model study of passive pressure in sand.'' *J. Soil Mech. Found. Div., Am. Soc. Civ. Eng.*, 95(4), 969–983.

Rowe, P. W., and Peaker, K. (1965). ''Passive earth pressure measurements.'' *Geotechnique*, 15(1), 57–78.

Schofield, A. N. (1961). ''The development of lateral force of sand against the vertical face of a rotating model foundation.'' *Proc., 5th Int. Conf. Soil Mechianics*, Paris, 479–484.

Sokolovski, V. V. (1960). *Statics of soil media*, Butterworths, London.

Tatsuoka, F., and Haibara, O. (1985). ''Shear resistance between sand and smooth or lubricated surface.'' *Soils Found.*, 25(1), 89–98.

Terzaghi, K. (1941). ''General wedge theory of earth pressure.'' *ASCE Trans.*, 106, 68–80.

Terzaghi, K. and Peck, R. B. (1967). *Soil mechanics in engineering practice*, 2nd Ed., Wiley, New York.

Terzaghi, K., Peck, R. B., and Mezri, G. (1996). *Soil mechanics in engineering practice*, 3rd Ed., Wiley, New York.

Uesugi, M., and Kishida, H. (1986). ''Influential factors of friction between steel and dry sands,'' *Soils Found.*, 26(2), 33–46.

U.S. Navy (1982). ''Foundations and earth structures.'' *NAVFAC Design Manual DM-7.2*, Naval Facilities Engineering Command, U.S. Government Printing Office, Washington, D.C.

Wu, B. F. (1992a). ''Design and construction of National Chiao Tung University model retaining wall.'' MS thesis, National Chiao Tung Univ., Hsinchu, Taiwan.

Wu, J. T. H. (1992b). ''Construction and Instrumentation of the Denver walls.'' *Proc., International Symposium on Geosynthetic Reinforced Soil Retaining Walls*, Balkema, Rotterdam, The Netherlands, 21–30.

J. Geotech. Geoenviron. Eng. 2002.128:651-659.